Journal of Thermal Analysis and Calorimetry (2019) 137:461–471
https://doi.org/10.1007/s10973-018-7957-5

Thermal degradation properties of LDPE insulation for new and aged fine wires

Zhi Wang[1] · Ruichao Wei[1] · Xiaoyao Ning[1] · Tian Xie[1] · Jian Wang[1]

Received: 18 August 2018 / Accepted: 27 November 2018 / Published online: 3 December 2018

Abstract
The thermal behavior of new and aged low-density polyethylene (LDPE) insulations was investigated using an SDT Q600 thermal analyzer. The activation energy and pyrolysis reaction model were estimated using the non-isothermal and masterplots methods. The thermal degradation processes present different behaviors of the LDPE insulations before and after thermal aging. The thermogravimetric curves shift to the direction of higher temperature, for the aged LDPE insulation. The values of activation energy evaluated using the Kissinger–Akahira–Sunose (KAS) and Flynn–Wall–Ozawa (FWO) methods are almost same. However, the activation energy values estimated by the Friedman method were slightly higher than those obtained using the KAS and FWO methods. The suitable pyrolysis reaction models of the new and aged LDPE insulations were attributed to the "Contracting area" (R2) model, which was determined using the generalized masterplots method. In addition, the pre-exponential factor and compensation effect are discussed. Finally, it should be stressed that the aged LDPE insulation generally pyrolyzes more weakly and with more difficulty than the new insulation, i.e., the ignition and flame spread of aged wire in old buildings are not relatively easy.

Keywords Fine wire · Thermal aging · Thermal analysis · Pyrolysis kinetics

Introduction

Polyethylene (PE) has a wide range of applications in society, such as in sheaths, insulation, pipeline, medicine, automobiles. [1, 2]. Particularly, low-density polyethylene (LDPE) is extensively processed into wire insulation, cable insulation, and cable sheaths, due to its excellent properties of moldability, electrical insulation, and chemical stability. Electrical wire or cable is a potential ignition source, and its polymer insulations or sheaths are important combustible materials in electrical fires [3, 4]. A large number of fire accidents related to electrical wires are reported annually [5]. Thermal degradation is the primary step in all thermochemical processes, including fires [6, 7]. It can be described as the pyrolysis of original materials into different phase/state products in an inert environment [8]. Therefore, the thermal degradation of wire insulation is significantly critical and must be paid much attention. A laboratory fine wire coated with LDPE insulation was used in this work, owing to the complicated fundamental study of actual wire insulation pyrolysis.

Many studies on the pyrolysis characteristics of polyethylene have been conducted using the thermogravimetric analysis (TGA) technique [9–16]. Cho et al. [11] investigated the pyrolysis kinetic parameters of LDPE and XLPE, using TGA and the Kissinger equation. They predicted the activation energy of LDPE and XLPE to be 146.8 and 170.4 kJ mol^{-1}, respectively. Park et al. [13] studied the thermal degradation of polymers, using the TGA technique, and obtained activation energies of 333.2–343.2 kJ mol^{-1}, 187.5–199.1 kJ mol^{-1}, and 219.2–230.1 kJ mol^{-1} for HDPE, LDPE, and LLDPE, respectively. Encinar et al. [17] conducted non-isothermal TGA at heating rates of 5, 10, 15, and 20 K min^{-1} on LDPE, and determined activation energies of 220–259 kJ mol^{-1}. Aboulkas et al. [15] performed TGA of HDPE and LDPE, at different heating rates (2, 10, 20, and 50 K min^{-1}) in the temperature range 300–900 K, under

✉ Jian Wang
wangj@ustc.edu.cn

[1] State Key Laboratory of Fire Science, University of Science and Technology of China, Hefei 230026, Anhui, People's Republic of China

nitrogen atmosphere. It was reported that the pyrolysis reaction models of HDPE and LDPE can be described using the R2 model, with activation energies of 238–247 and 215–221 kJ mol^{-1}, respectively. For the wire or cable insulation and sheath, Beneš et al. [18], Henrist et al. [19], Xie et al. [3], Mo et al. [20], and Wang et al. [4] studied the thermal degradation characteristics of PVC sheaths and XLPE insulations. Sebaa et al. [21], Nedjar [22], Wang et al. [23], Boukezzi et al. [24], and Geng et al. [25] conducted the most studies focusing on the effect of thermal aging on electrical and mechanical characteristics. However, limited work was done to analyze the thermal degradation properties of LDPE insulation for new and aged wires, with regard to fire risk.

In this study, several thermogravimetry experiments were carried out on the LDPE insulation of new and aged fine wires, at different heating rates, to explore the thermal degradation properties. The non-isothermal and master-plots methods were used to calculate the activation energy and determine the pyrolysis reaction model for the new and aged LDPE insulations. The effect of thermal aging on the pyrolysis process of the LDPE insulations is discussed.

Materials and experimental procedure

Materials

The fine wire consisted of a copper core and polymer insulation and had an external diameter of 0.80 mm and an insulation thickness of 0.15 mm. The samples used in this work were the polymer insulations taken from new and aged fine wires. The main components of the polymer insulations were LDPE and additives. There was no flame retardant in the polymer insulations. Before the tests, all the samples were dried at 60 °C for 24 h, to remove moisture.

Experimental

Aging procedure

The fine wires were aged in an air-circulation oven (GHX-100L, Hefei Anke Environmental Test Equipment Co. Ltd, Hefei City, China). The wire samples were cut into several parts with a length of 200 mm and were hung below a steel grid with enough space to ensure that the circulated air passed through and around each sample without restriction. The preset temperature in the oven was 90 ± 0.1 °C. The wire samples were removed from the oven at certain time intervals of 0, 15, and 32 days (LDPE-0, LDPE-15, and LDPE-32), respectively. Thereafter, the removed samples were stored under constant conditions (a temperature of 25 °C and humidity of 60%) until the thermal degradation properties could be further studied using a thermal analyzer.

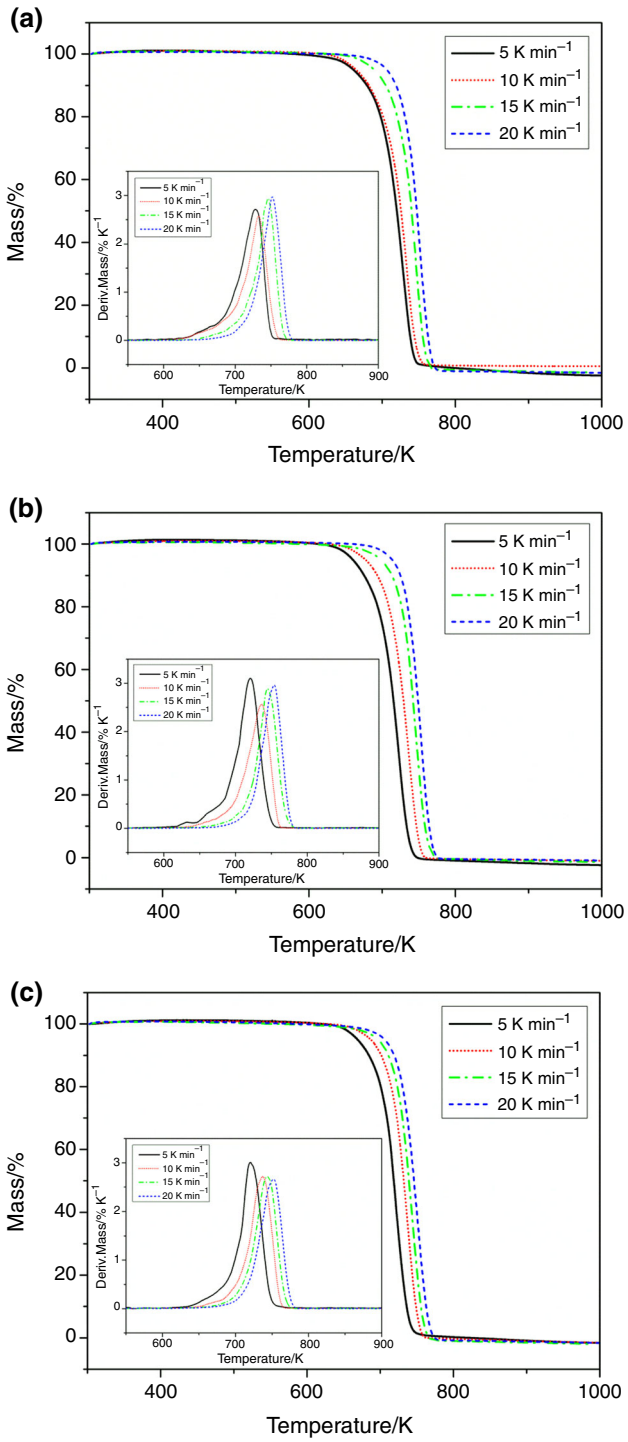

Fig. 1 TG curves (inset: DTG curves) for different heating rates under nitrogen atmosphere: **a** LDPE-0, **b** LDPE-15, and **c** LDPE-32

TGA procedure

A TA Instruments SDT Q600 thermal analyzer was employed to monitor the whole decomposition process. 5 ± 0.2 mg of the sample was placed into an alumina crucible, in each test. All the experiments were conducted under nitrogen atmosphere, with a flow rate of 50 mL min^{-1}. For the thermal degradation of a cable sheath and insulation, Beneš et al. [18] considered five heating rates of 1.5, 5, 10, 15, and 20 K min^{-1}, in the temperature range 20–800 °C. Xie et al. [3] conducted thermogravimetry experiments at 5, 15, 25, and 35 K min^{-1}, from room temperature to a temperature more than 1000 K. Wang et al. [4] also chose five heating rates of 10, 20, 30, 40, and 50 K min^{-1}, and the test temperature range was 300–1200 K. Therefore, the samples were heated from room temperature to 800 °C, at four heating rates of 5, 10, 15, and 20 K min^{-1}.

Results and discussion

Thermal degradation

Figure 1a–c shows the profiles of relative mass loss (TG) and mass loss rate (DTG) of the new and aged LDPE

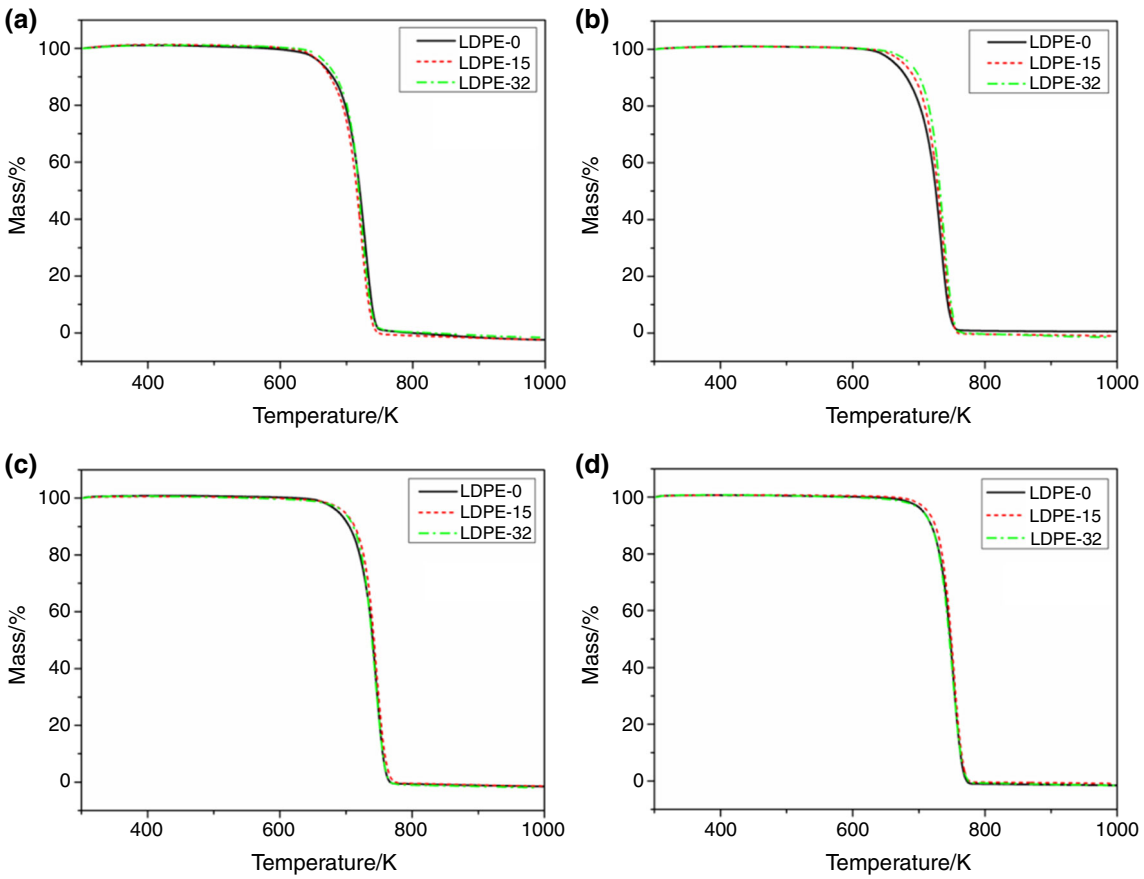

Fig. 2 Comparison of TG of LDPE insulation for new and aged wires under nitrogen atmosphere: **a** 5 K min^{-1}, **b** 10 K min^{-1}, **c** 15 K min^{-1}, and **d** 20 K min^{-1}

Table 1 Pyrolysis parameters of LDPE insulation

Heating rate/K min^{-1}	LDPE-0			LDPE-15			LDPE-32		
	pDTG/% K^{-1}	pT/K	rMass/%	pDTG/% K^{-1}	pT/K	rMass/%	pDTG/% K^{-1}	pT/K	rMass/%
5	2.74	726.7	2.76	3.10	726.9	2.66	3.04	727.3	1.73
10	2.61	732.7	0.59	2.60	736.3	1.23	2.77	737.1	1.73
15	2.98	745.2	1.78	2.92	745.5	1.62	2.76	746.3	2.19
20	2.96	750.6	1.74	2.99	752.7	1.09	2.69	754.7	1.88

insulations under nitrogen atmosphere, for different heating rates of 5–20 K min^{-1}. The TG and DTG curves show almost the same trend, regardless of the heating rate, which indicates that the samples underwent a similar pyrolysis process due to the similar chemical bonds in their molecular structures. The thermal degradation of LDPE is generally considered to be a one-step process [15, 16, 26, 27]. This can be confirmed by the presence of only a single step in the TG curve and a single DTG peak. This could be attributed to the random cleavage of the chains and the formation of free radicals [2]. As the heating rate increased, it should be noted that there was a lateral shift to a higher temperature in the TG and DTG curves. This phenomenon has been described and explained by different researchers [10, 13, 15, 28].

A comparison of the TG curves of the LDPE insulations of new and aged wires is presented in Fig. 2a–d. The onset and peak temperatures from the DTG (pT) of the pyrolysis process, corresponding to LDPE-15 and LDPE-32, are slightly higher than those of LDPE-0, regardless of the heating rate. Differences in the peak DTG (pDTG) and residue mass (rMass) between the new and aged wire insulations were also observed. In other words, the pyrolysis differences between the new and aged wire insulations were all similar when the heating rates were 5, 10, 15, and 20 K min^{-1}. The pyrolysis parameters of LDPE-0, LDPE-15, and LDPE-32 are listed in Table 1. All these results show that the aged wire insulation starts to pyrolyze with more difficulty, which suggests that the active chemical composition and structure of the LDPE insulation decomposed, and was released during thermal aging.

Determination of activation energy

In this work, some commonly used isoconversional methods of Kissinger–Akahira–Sunose (KAS) [29, 30], Flynn–Wall–Ozawa (FWO) [31, 32], and Friedman [16, 33, 34] were employed to calculate the activation energy. The KAS method can be represented as follows:

$$\ln\frac{\beta}{T^2} = \ln\left(\frac{AR}{E_\alpha g(\alpha)}\right) - \frac{E_\alpha}{RT} \quad (1)$$

where $\beta = dT/dt$ is the heating rate (K s^{-1}); A is the pre-exponential factor (s^{-1}); R is the universal gas constant (8.314 J mol^{-1} K^{-1}); E_α is the activation energy of the reaction (J mol^{-1}); T is the absolute temperature; and $g(\alpha)$ is an integral function of the conversion, which can be written as:

$$g(\alpha) = \int_0^\alpha \frac{d\alpha}{f(\alpha)} = \frac{A}{\beta}\int_{T_0}^{T} \exp\left(-\frac{E_\alpha}{RT}\right)dT \quad (2)$$

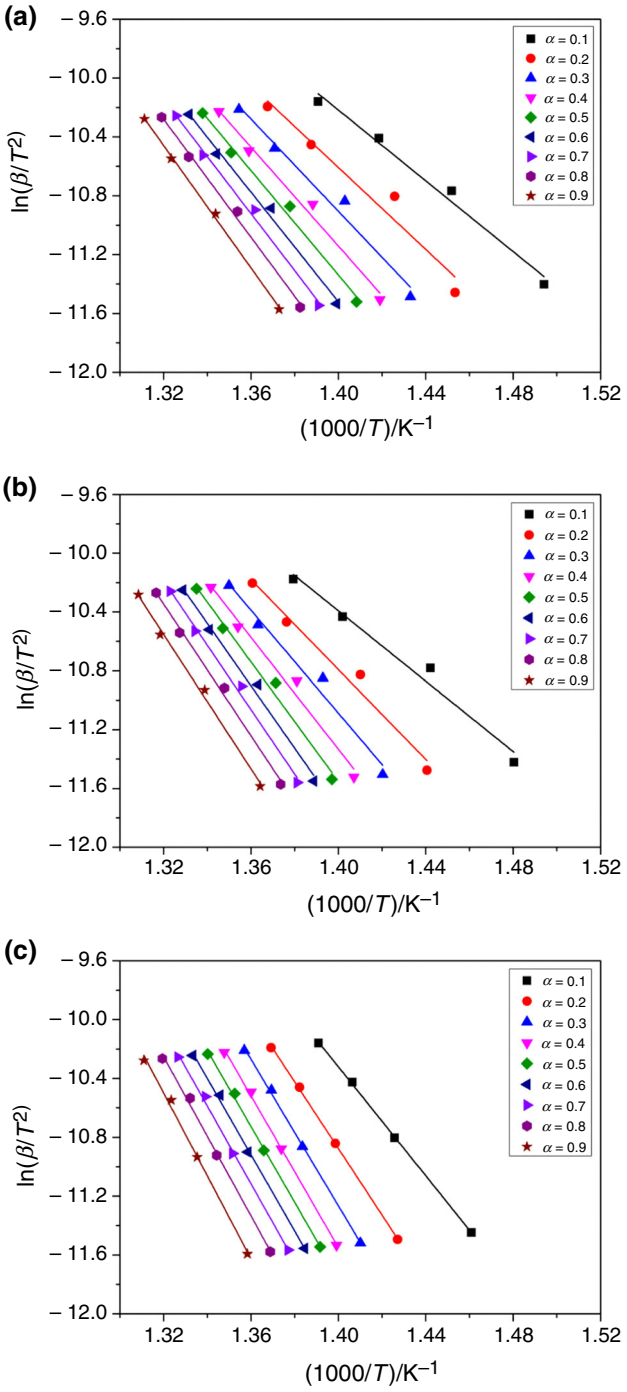

Fig. 3 KAS plots for various conversion rates: **a** LDPE-0, **b** LDPE-15, and **c** LDPE-32

where α is the conversion rate and can be defined as $\alpha = (m_i - m_t)/(m_i - m_f)$. m_i, m_t, and m_f are the initial mass, the mass at time t, and the mass after the reaction, respectively. $f(\alpha)$ is the function of conversion. The conversion rate was chosen between 0.1 and 0.9, with a step size of 0.1 under different heating rates.

Table 2 Activation energy values obtained using the KAS method

LDPE-0			LDPE-15			LDPE-32		
α	E_α/kJ mol^{-1}	R^2	α	E_α/kJ mol^{-1}	R^2	α	E_α/kJ mol^{-1}	R^2
0.1	130.04 ± 5	0.979	0.1	139.45 ± 15	0.967	0.1	173.95 ± 12	1
0.2	140.84 ± 7	0.933	0.2	151.05 ± 13	0.967	0.2	208.27 ± 8	0.999
0.3	150.32 ± 4	0.969	0.3	165.51 ± 8	0.970	0.3	227.01 ± 10	0.999
0.4	159.80 ± 6	0.981	0.4	178.07 ± 10	0.975	0.4	234.54 ± 9	0.998
0.5	167.54 ± 7	0.987	0.5	188.95 ± 6	0.982	0.5	234.53 ± 7	0.998
0.6	175.09 ± 11	0.991	0.6	196.44 ± 9	0.987	0.6	235.67 ± 13	0.997
0.7	181.24 ± 9	0.992	0.7	202.23 ± 5	0.990	0.7	239.80 ± 12	0.996
0.8	186.83 ± 8	0.994	0.8	206.39 ± 8	0.993	0.8	245.01 ± 7	0.995
0.9	193.10 ± 13	0.998	0.9	209.94 ± 11	0.992	0.9	254.48 ± 6	0.994

Hence, E_a can be obtained from the slope of the straight line between $\ln(\beta/T^2)$ and $1/T$. Figure 3a–c presents the plots of $\ln(\beta/T^2)$ against $1000/T$ for different conversion rates of the new and aged LDPE insulations. The values of E_α estimated using the isoconversional KAS method are

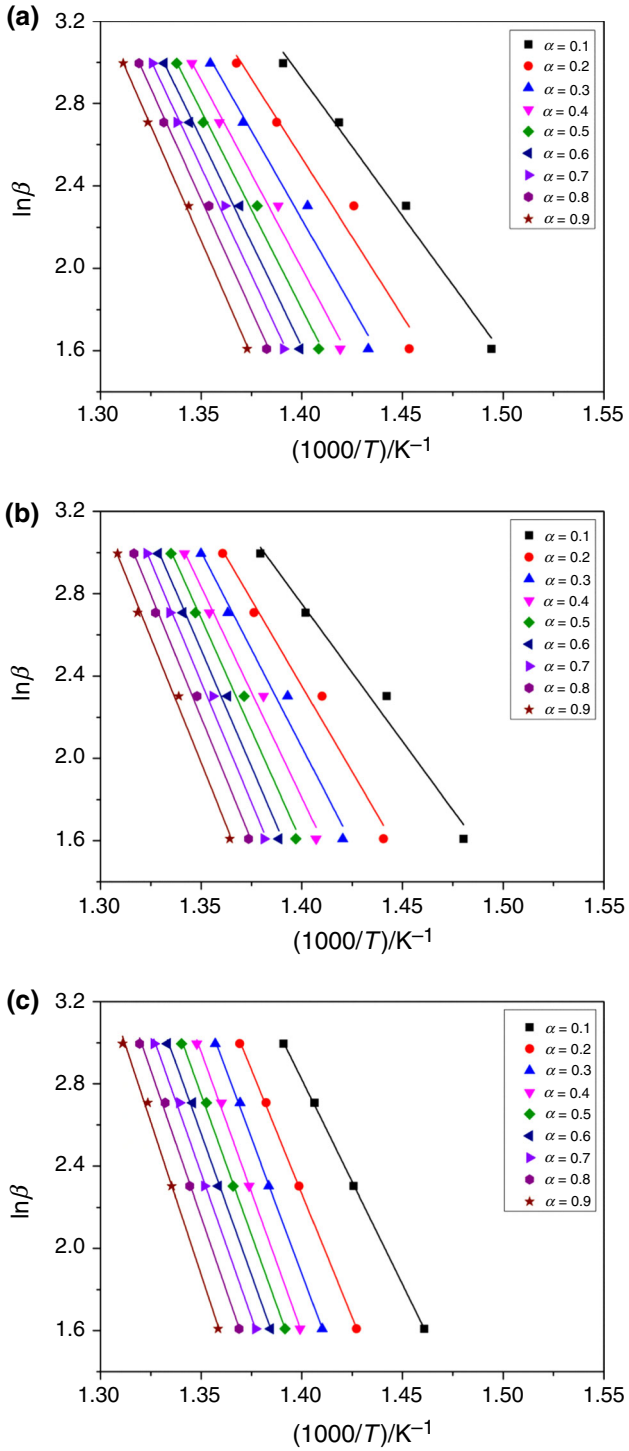

Fig. 4 FWO plots for various conversion rates: **a** LDPE-0, **b** LDPE-15, and **c** LDPE-32

shown in Table 2, for LDPE-0, LDPE-15, and LDPE-32. It was found that the E_α first increases and then tends to stabilize with an increase in the α. The E_α of LDPE-32 is higher than that of LDPE-15, and LDPE-0 has the lowest E_α under the same conversion rate. The mean values of E_α were 164.98, 182.00, and 228.14 kJ mol^{-1} for LDPE-0, LDPE-15, and LDPE-32, respectively.

The FWO method is derived from the integral isoconversional method. Based on Doyle's approximation [35], the FWO method can be expressed as:

$$\ln \beta = \ln \frac{\mathrm{AE}_\alpha}{\mathrm{Rg}(\alpha)} - 5.331 - 1.052 \frac{E_\alpha}{\mathrm{RT}} \tag{3}$$

Therefore, the plot of lnβ versus $1/T$ should be a straight line, whose slope can be applied to evaluate the activation energy of the reaction. Figure 4a–c shows the plots of lnβ as a function of 1000/T for various conversion rates of the new and aged LDPE insulations. The activation energy values calculated using the FWO method are listed in Table 3, for LDPE-0, LDPE-15, and LDPE-32. The value of E_α ranges 135.09–196.38 kJ mol^{-1}, with an average value of 169.08 kJ mol^{-1}, for LDPE-0; 146.63–212.45 kJ mol^{-1}, with an average value of 185.71 kJ mol^{-1}, for LDPE-15; and 177.47–254.82 kJ mol^{-1}, with an average value of 229.46 kJ mol^{-1}, for LDPE-32.

The Friedman method is a common differential isoconversional method [34], whose logarithm equation is frequently used in the following form [36]:

$$\ln\left(\frac{\mathrm{d}\alpha}{\mathrm{d}t}\right) = \ln\left(\beta \frac{\mathrm{d}\alpha}{\mathrm{d}T}\right) = \ln[f(\alpha)A] - \frac{E_\alpha}{\mathrm{RT}} \tag{4}$$

By plotting $\ln[\beta(\mathrm{d}\alpha/\mathrm{d}T)]$ against $1/T$ for the whole range of conversions (0.1–0.9), the activation energy can be determined from the slope. Figure 5a–c depicts the plots for the determination of E_α at different conversion rates under nitrogen atmosphere. The E_α estimated using the Friedman method is presented in Table 3, for LDPE-0, LDPE-15, and LDPE-32. The activation energy values were 139.19–205.09 kJ mol^{-1} for LDPE-0, 159.45–221.92 kJ mol^{-1} for LDPE-15, and 207.11–269.95 kJ mol^{-1} for LDPE-32, under different conversion rates. The mean values of the activation energy are 185.10, 205.46, and 237.49 kJ mol^{-1} for LDPE-0, LDPE-15, and LDPE-32, respectively.

The activation energy values for each α of LDPE-0, LDPE-15, and LDPE-32, based on the three isoconversional methods of two types (integral and differential), are summarized in Fig. 6. It is worth noting that a satisfactory agreement was found in the activation energy distribution, between the KAS and FWO methods, and their curves were almost overlapping, with less deviation. However, the activation energy values evaluated using the Friedman method were slightly higher than those obtained using the KAS and FWO methods. This could be ascribed to the different approximations used in the algorithms [36]. It is also evident that the values of the activation energy of the aged insulation are higher than those of the new insulation. It must be stressed that the LDPE insulation of the aged wire had a larger activation energy, resulting in poor pyrolysis. This parameter implies that the ignition of aged wires in fire is difficult (Table 4).

Determination of reaction mechanism

The reaction mechanism $f(\alpha)$ could be determined using the generalized Criado masterplots method [15, 16], expressed as follows:

$$\frac{Z(\alpha)}{Z(0.5)} = \frac{f(\alpha)g(g)}{f(0.5)g(0.5)} = \left(\frac{T_\alpha}{T_{0.5}}\right)^2 \frac{(\mathrm{d}\alpha/\mathrm{d}t)_\alpha}{(\mathrm{d}\alpha/\mathrm{d}t)_{0.5}} \tag{5}$$

Table 3 Activation energy values obtained using the FWO method

LDPE-0			LDPE-15			LDPE-32		
α	E_α/kJ mol^{-1}	R^2	α	E_α/kJ mol^{-1}	R^2	α	E_α/kJ mol^{-1}	R^2
0.1	135.09 ± 11	0.984	0.1	146.63 ± 8	0.974	0.1	177.47 ± 13	1
0.2	144.37 ± 13	0.945	0.2	155.10 ± 15	0.972	0.2	210.33 ± 9	1
0.3	155.27 ± 10	0.974	0.3	169.79 ± 11	0.974	0.3	228.27 ± 11	0.999
0.4	164.38 ± 9	0.984	0.4	181.82 ± 13	0.978	0.4	235.52 ± 7	0.998
0.5	171.81 ± 12	0.989	0.5	192.23 ± 8	0.985	0.5	235.57 ± 9	0.998
0.6	179.06 ± 8	0.992	0.6	199.42 ± 4	0.989	0.6	236.72 ± 6	0.997
0.7	184.97 ± 6	0.993	0.7	204.98 ± 7	0.991	0.7	240.70 ± 12	0.997
0.8	190.35 ± 7	0.995	0.8	208.99 ± 5	0.994	0.8	245.73 ± 8	0.996
0.9	196.38 ± 3	0.998	0.9	212.45 ± 9	0.993	0.9	254.82 ± 10	0.995

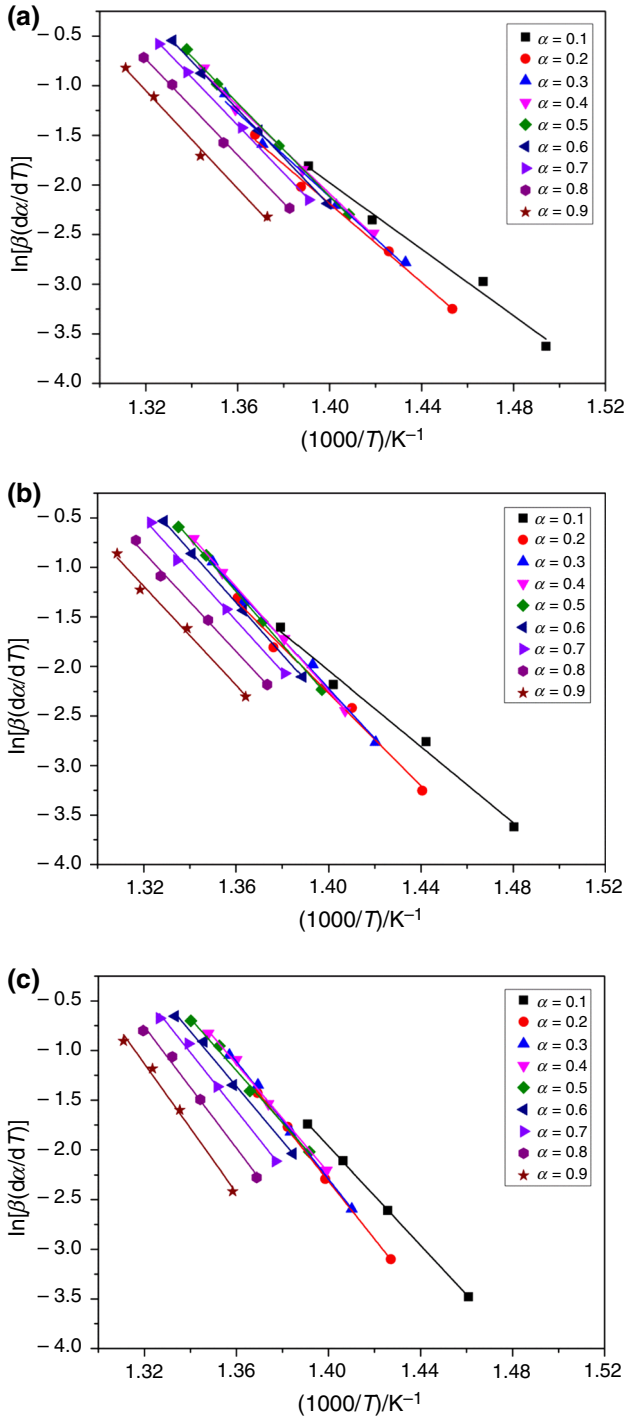

Fig. 5 Friedman plots for various conversion rates: **a** LDPE-0, **b** LDPE-15, and **c** LDPE-32

where $(d\alpha/dt)_{0.5}$ and $T_{0.5}$ are the conversion rate and temperature corresponding to $\alpha = 0.5$, respectively. The left side of Eq. (5) is the theoretical masterplot that signifies the characteristics of each reaction mechanism described in Table 5, whereas the right side of the equation, associated with the reduced rate, can be obtained from experimental data. For multiple heating-rate data, the masterplots must be obtained for all the heating rates, and the most suitable model is selected based on the agreement between the theoretical masterplots and experimental reduced rate plots.

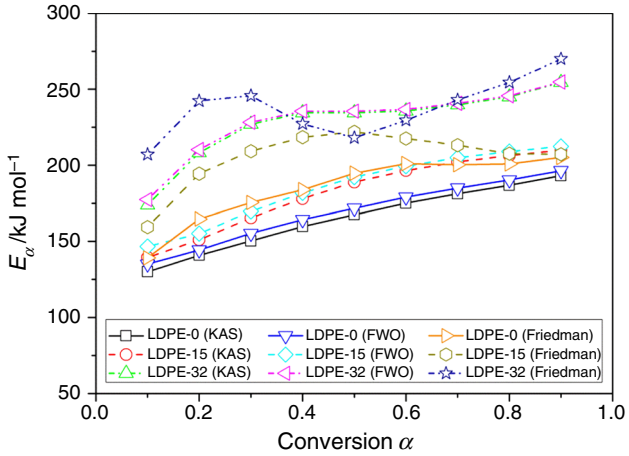

Fig. 6 Dependence of activation energy on the conversion α for thermal degradation of LDPE, according to the KAS, FWO, and Friedman methods

Figure 7 presents the masterplots of various kinetic models and experimental data for different heating rates of the new and aged LDPE insulations. As shown in Fig. 7, the "Contracting area" model (R2), with a better fitting degree, is more appropriate to describe the thermal degradation process of the LDPE materials used in this study; this is basically consistent with earlier studies [16]. However, it should be noted that the experimental masterplots slightly deviate from the theoretical masterplots when the conversation rate is above 0.5, and this deviation is pronounced for the aged LDPE insulation. This indicates that the whole degradation process is complex, involving successive, parallel, and/or reversible reactions, diffusion, etc. This could be ascribed to the changes in chemical composition and structure inside the materials, after thermal aging, leading to a variation in the reaction mechanism.

The pre-exponential factor A can be estimated using the Constable plot [37], also known as the compensation method [34], after the reaction mechanism $f(\alpha)$ is determined. In a more generalized form, the relationship between E_α and $\ln A_\alpha$ can be written as [36, 38]:

Table 4 Activation energy values obtained using the Friedman method

LDPE-0			LDPE-15			LDPE-32		
α	E_α/kJ mol^{-1}	R^2	α	E_α/kJ mol^{-1}	R^2	α	E_α/kJ mol^{-1}	R^2
0.1	139.19 ± 16	0.980	0.1	159.45 ± 13	0.985	0.1	207.11 ± 14	1
0.2	164.83 ± 14	0.992	0.2	194.53 ± 10	0.986	0.2	242.37 ± 10	0.999
0.3	175.58 ± 11	0.986	0.3	209.26 ± 9	0.993	0.3	245.68 ± 12	0.997
0.4	183.96 ± 9	0.994	0.4	218.41 ± 11	0.999	0.4	227.22 ± 9	0.996
0.5	194.80 ± 10	0.999	0.5	221.92 ± 8	0.999	0.5	218.08 ± 11	0.991
0.6	201.12 ± 7	1	0.6	217.62 ± 5	1	0.6	229.52 ± 7	0.993
0.7	200.38 ± 5	1	0.7	213.19 ± 7	0.995	0.7	243.02 ± 10	0.992
0.8	200.91 ± 8	0.999	0.8	207.57 ± 3	0.994	0.8	254.48 ± 8	0.990
0.9	205.09 ± 6	0.992	0.9	207.24 ± 8	0.987	0.9	269.95 ± 5	0.987

Table 5 Algebraic expressions of common reaction mechanisms

Model	$f(\alpha)$	$g(\alpha)$
P2 Power law	$2\alpha^{1/2}$	$\alpha^{1/2}$
P3 Power law	$3\alpha^{2/3}$	$\alpha^{1/3}$
P4 Power law	$4\alpha^{3/4}$	$\alpha^{1/4}$
A2 Avrami–Erofeev	$2(1-\alpha)[-\ln(1-\alpha)]^{1/2}$	$[-\ln(1-\alpha)]^{1/2}$
A3 Avrami–Erofeev	$3(1-\alpha)[-\ln(1-\alpha)]^{2/3}$	$[-\ln(1-\alpha)]^{1/3}$
A4 Avrami–Erofeev	$4(1-\alpha)[-\ln(1-\alpha)]^{3/4}$	$[-\ln(1-\alpha)]^{1/4}$
R2 Contracting area	$2(1-\alpha)^{1/2}$	$\left[1-(1-\alpha)^{1/2}\right]$
R3 Contracting volume	$3(1-\alpha)^{2/3}$	$\left[1-(1-\alpha)^{1/3}\right]$
D1 One-dimensional diffusion	$1/2\alpha^{-1}$	α^2
D2 Two-dimensional diffusion	$[-\ln(1-\alpha)]^{-1}$	$[(1-\alpha)\ln(1-\alpha)]+\alpha$
D3 Three-dimensional diffusion—Jander	$3/2(1-\alpha)^{2/3}\left[1-(1-\alpha)^{1/3}\right]^{-1}$	$\left[1-(1-\alpha)^{1/3}\right]^2$
D4 Three-dimensional diffusion—Ginstling	$3/2\left[(1-\alpha)^{-1/3}-1\right]$	$1-2\alpha/3-(1-\alpha)^{2/3}$
F1 First order	$1-\alpha$	$-\ln(1-\alpha)$
F2 Second order	$(1-\alpha)^2$	$(1-\alpha)^{-1}-1$
F3 Third order	$(1-\alpha)^3$	$\left[(1-\alpha)^{-2}-1\right]/2$

$$\ln A_\alpha = aE_\alpha + b \tag{6}$$

where a and b are constants known as the compensation effect parameters. In this relationship, E_α and $\ln A_\alpha$ are in a good linear correlation. Hence, a change in E_α due to the experimental factors must make the $\ln A_\alpha$ change accordingly. The values of E_α and $\ln A_\alpha$ are listed in Table 6, and the corresponding fitted lines are shown in Fig. 8. The fitted line of the new LDPE insulation is almost in agreement with that of the aged insulation. Therefore, it can be concluded that thermal aging has little influence on the compensation effect parameters of the LDPE insulations used in this study. The linear fit of the three LDPE insulation samples can be expressed as:

$$\ln A_\alpha = 0.165E_\alpha - 1.916; R^2 = 0.999 \tag{7}$$

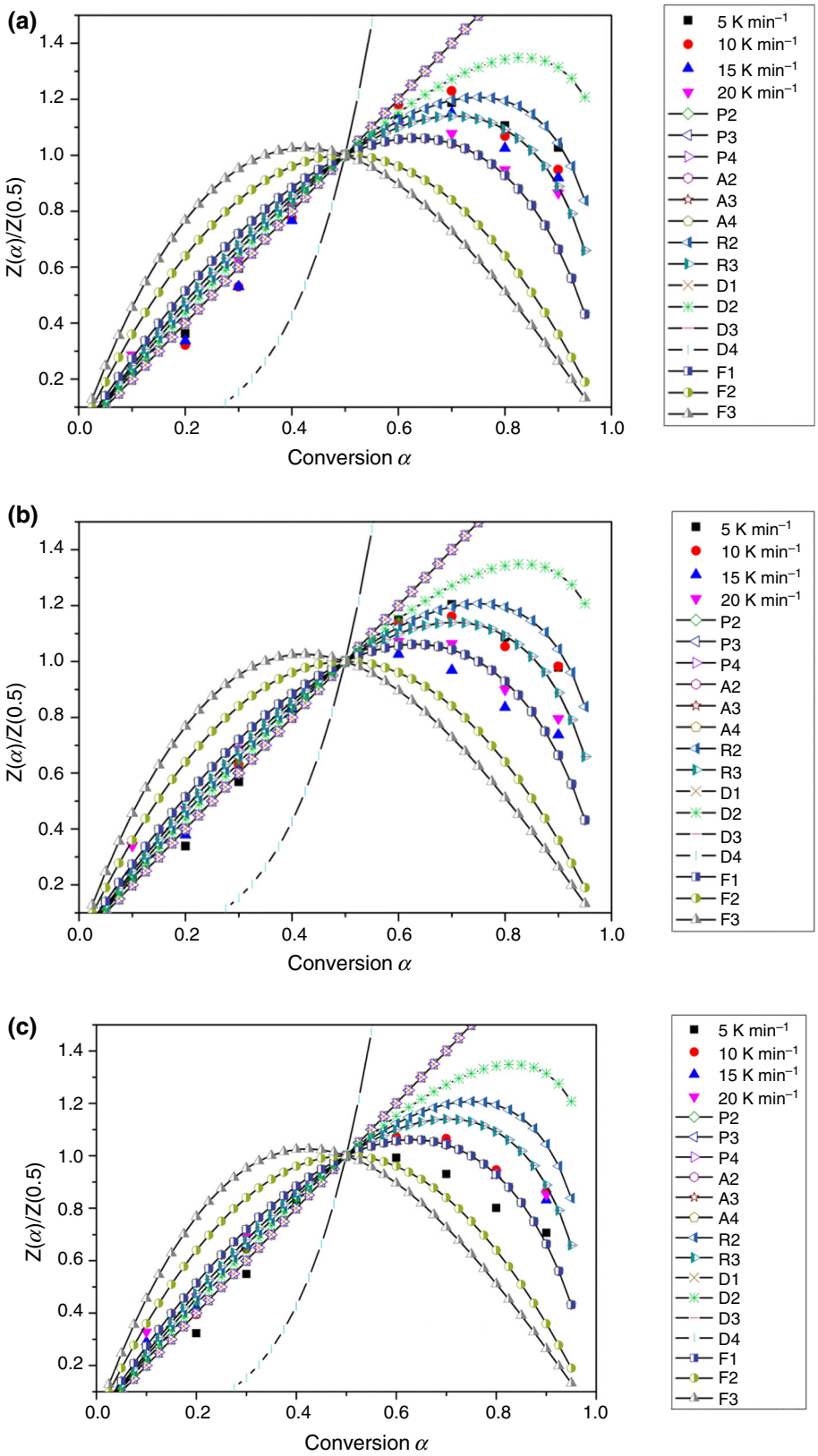

Fig. 7 Theoretical masterplots for different reaction models, and experimental reduced rate plots for different heating rates: **a** LDPE-0, **b** LDPE-15, and **c** LDPE-32

Table 6 E_α and $\ln A_\alpha$ values for new and aged LDPE insulations for different conversion rates

Conversion rate (α)	LDPE-0		LDPE-15		LDPE-32	
	E_α /kJ mol^{-1}	$\ln A_\alpha$/ln s^{-1}	E_α /kJ mol^{-1}	$\ln A_\alpha$/ln s^{-1}	E_α /kJ mol^{-1}	$\ln A_\alpha$/ln s^{-1}
0.1	139.19	20.82	159.45	24.16	207.11	32.27
0.2	164.83	24.99	194.53	29.90	242.37	37.92
0.3	175.58	26.94	209.26	32.50	245.68	38.56
0.4	183.96	28.45	218.41	34.09	227.22	35.59
0.5	194.80	30.35	221.92	34.72	218.08	34.13
0.6	201.12	31.43	217.62	34.01	229.52	35.95
0.7	200.38	31.29	213.19	33.24	243.02	38.05
0.8	200.91	31.28	207.57	32.22	254.48	39.76
0.9	205.09	31.97	207.24	32.18	269.95	42.19

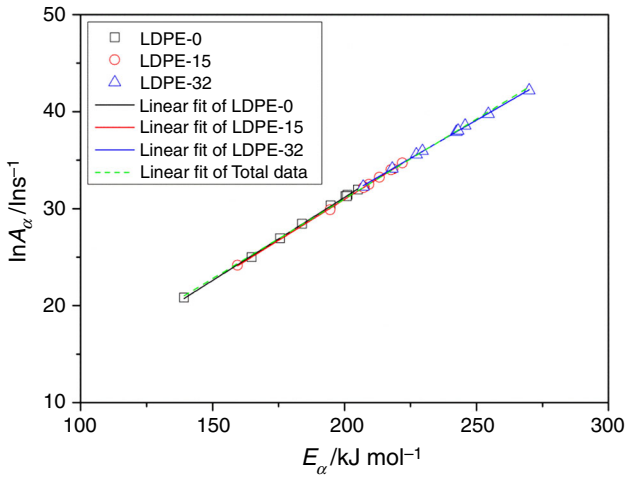

Fig. 8 Compensation effect for the three LDPE insulations

Conclusions

In this study, a series of thermogravimetry experiments were carried out for LDPE insulations of new and aged fine wires, at different heating rates of 5–20 K min^{-1} under nitrogen atmosphere. The displacement of the whole TG and DTG curves for the aged LDPE insulation tends to the direction of higher temperature, regardless of the change in heating rate. The activation energy was evaluated using three isoconversional methods (KAS, FWO, and Friedman), for various conversion rates. The results illustrate that the activation energy of the LDPE insulation after thermal aging is clearly higher than that of the new insulation. The masterplots method was utilized to obtain the reaction mechanisms of the new and aged LDPE insulations. The pre-exponential factor was also calculated. The thermal degradation models of LDPE-0, LDPE-15, and LDPE-32 could be described using the R2 model, in this work. The relationship of the compensation effect for the three samples is identical. In addition, it could also be deduced that the LDPE insulation of aged wire is harder to pyrolyze and tougher to ignite. However, more gaseous products in decomposition, ignition, and combustion tests are needed as the next step to verify the conclusions of this work. Actually, the fire risk for electric wires or cables is more related to electrical failures (including overloads, short circuits, poor contacts). In such cases, thermo-oxidative aging plays a major role in the lifetime limitation of cables by deteriorating both the mechanical and electrical properties. These are also worth studying in the future.

Acknowledgements This work was supported by the National Key R&D Program of China (No. 2018YFC0809500). The authors gratefully acknowledge this support.

References

1. Peacock A. Handbook of polyethylene: structures—properties, and applications. Boca Raton: CRC Press; 2000.
2. Oluwoye I, Altarawneh M, Gore J, Dlugogorski BZ. Oxidation of crystalline polyethylene. Combust Flame. 2015;162(10):3681–90.
3. Xie Q, Zhang H, Tong L. Experimental study on the fire protection properties of PVC sheath for old and new cables. J Hazard Mater. 2010;179(1–3):373–81.
4. Wang C, Liu H, Zhang J, Yang S, Zhang Z, Zhao W. Thermal degradation of flame-retarded high-voltage cable sheath and insulation via TG-FTIR. J Anal Appl Pyrolysis. 2018;11:1997.
5. He H, Zhang Q, Tu R, Zhao L, Liu J, Zhang Y. Molten thermoplastic dripping behavior induced by flame spread over wire insulation under overload currents. J Hazard Mater. 2016;320:628–34.
6. Wang G, Li W, Li B, Chen H. TG study on pyrolysis of biomass and its three components under syngas. Fuel. 2008;87(4–5):552–8.
7. Ding Y, Ezekoye OA, Lu S, Wang C, Zhou R. Comparative pyrolysis behaviors and reaction mechanisms of hardwood and softwood. Energ Convers Manage. 2017;132:102–9.
8. Martın-Gullon I, Esperanza M, Font R. Kinetic model for the pyrolysis and combustion of poly-(ethylene terephthalate)(PET). J Anal Appl Pyrolysis. 2001;58:635–50.

9. Anderson DA, Freeman ES. The kinetics of the thermal degradation of polystyrene and polyethylene. J Polym Sci Part A Polym Chem. 1961;54(159):253–60.
10. Conesa JA, Marcilla A, Font R, Caballero JA. Thermogravimetric studies on the thermal decomposition of polyethylene. J Anal Appl Pyrolysis. 1996;36(1):1–15.
11. Cho Y-S, Shim M-J, Kim S-W. Thermal degradation kinetics of PE by the Kissinger equation. Mater Chem Phys. 1998;52(1):94–7.
12. Bockhorn H, Hornung A, Hornung U, Schawaller D. Kinetic study on the thermal degradation of polypropylene and polyethylene. J Anal Appl Pyrolysis. 1999;48(2):93–109.
13. Park JW, Oh SC, Lee HP, Kim HT, Yoo KO. A kinetic analysis of thermal degradation of polymers using a dynamic method. Polym Degrad Stabil. 2000;67(3):535–40.
14. Aboulkas A, El Harfi K, El Bouadili A. Non-isothermal kinetic studies on co-processing of olive residue and polypropylene. Energ Convers Manage. 2008;49(12):3666–71.
15. Aboulkas A, El Bouadili A. Thermal degradation behaviors of polyethylene and polypropylene. Part I: pyrolysis kinetics and mechanisms. Energy Convers Manage. 2010;51(7):1363–9.
16. Das P, Tiwari P. Thermal degradation kinetics of plastics and model selection. Thermochim Acta. 2017;654:191–202.
17. Encinar JM, González JF. Pyrolysis of synthetic polymers and plastic wastes. Kinetic study. Fuel Process Technol. 2008;89(7):678–86.
18. Beneš M, Milanov N, Matuschek G, Kettrup A, Plaček V, Balek V. Thermal degradation of PVC cable insulation studied by simultaneous TG-FTIR and TG-EGA methods. J Therm Anal Calorim. 2004;78(2):621–30.
19. Henrist C, Rulmont A, Cloots R, Gilbert B, Bernard A, Beyer G. Toward the understanding of the thermal degradation of commercially available fire-resistant cable. Mater Lett. 2000;46(2–3):160–8.
20. Mo S-j, Zhang J, Liang D, Chen H-y. Study on pyrolysis characteristics of cross-linked polyethylene material cable. Proc Eng. 2013;52:588–92.
21. Sebaa M, Servens C, Pouyet J. Natural and artificial weathering of low-density polyethylene (LDPE): calorimetric analysis. J Appl Polym Sci. 1993;47(11):1897–903.
22. Nedjar M. Effect of thermal aging on the electrical properties of crosslinked polyethylene. J Appl Polym Sci. 2009;111(4):1985–90.
23. Wang Y, Wang C, Zhang Z, Xiao K. Effect of nanoparticles on the morphology, thermal, and electrical properties of low-density polyethylene after thermal aging. Nanomaterials. 2017;7(10):320.
24. Boukezzi L, Boubakeur A. Effect of thermal aging on the electrical characteristics of XLPE for HV cables. Trans Electr Electron Mater. 2018;19(5):344–51.
25. Geng P, Song J, Tian M, Lei Z, Du Y. Influence of thermal aging on AC leakage current in XLPE insulation. AIP Adv. 2018;8(2):025115.
26. Peterson JD, Vyazovkin S, Wight CA. Kinetics of the thermal and thermo-oxidative degradation of polystyrene, polyethylene and poly (propylene). Macromol Chem Phys. 2001;202(6):775–84.
27. Piiroja E, Lippmaa H, editors. Thermal degradation of polyethylene. Makromolekulare chemie. Macromolecular symposia. New York: Wiley; 1989.
28. Yang J, Miranda R, Roy C. Using the DTG curve fitting method to determine the apparent kinetic parameters of thermal decomposition of polymers. Polym Degrad Stabil. 2001;73(3):455–61.
29. Kissinger HE. Reaction kinetics in differential thermal analysis. Anal Chem. 1957;29(11):1702–6.
30. Akahira T, Sunose T. Method of determining activation deterioration constant of electrical insulating materials. Res Rep Chiba Inst Technol (Sci Technol). 1971;16:22–31.
31. Ozawa T. A new method of analyzing thermogravimetric data. Bull Chem Soc Jpn. 1965;38(11):1881–6.
32. Flynn JH, Wall LA. A quick, direct method for the determination of activation energy from thermogravimetric data. J Polym Sci Part C: Polym Lett. 1966;4(5):323–8.
33. Brown M, Maciejewski M, Vyazovkin S, Nomen R, Sempere J, Aa Burnham, et al. Computational aspects of kinetic analysis: Part A—the ICTAC kinetics project-data, methods and results. Thermochim Acta. 2000;355(1–2):125–43.
34. Vyazovkin S, Burnham AK, Criado JM, Pérez-Maqueda LA, Popescu C, Sbirrazzuoli N. ICTAC Kinetics Committee recommendations for performing kinetic computations on thermal analysis data. Thermochim Acta. 2011;520(1–2):1–19.
35. Doyle CD. Kinetic analysis of thermogravimetric data. J Appl Polym Sci. 1962;6(19):239–51.
36. Xu L, Jiang Y, Wang L. Thermal decomposition of rape straw: Pyrolysis modeling and kinetic study via particle swarm optimization. Energy Convers Manage. 2017;146:124–33. https://doi.org/10.1016/j.enconman.2017.05.020.
37. Tiwari P, Deo M. Detailed kinetic analysis of oil shale pyrolysis TGA data. AIChE J. 2012;58(2):505–15.
38. Wei R, He Y, Zhang Z, He J, Yuen R, Wang J. Effect of different humectants on the thermal stability and fire hazard of nitrocellulose. J Therm Anal Calorim. 2018;1:1–17.